

Analysis of Styrene Polymerization Without Surfactant and N₂ Gas in Cylindrical Flask

*Antony Ernesto dos Santos Silva^a, Wagner Cirilo Rodrigues^b, Walker de Lima Cordeiro^c,
Phabyanno Rodrigues Lima^{a,c}, Jonas dos Santos Sousa^a, Alan John Duarte de Freitas^a,
Johnnatan Duarte de Freitas^a, Djalma de Albuquerque Barros Filho^{a*}*

^aInstituto Federal de Alagoas- IFAL, Rua Mizaél Domingues, 75, Centro, Zip-Code: 57020-600, Maceió, AL, Brazil

^bInstituto Federal de Alagoas - IFAL, Rua da Matança, 176, Poeira, Zip-Code: 57160-000, Marechal Deodoro, AL, Brazil

^cUniversidade Federal de Alagoas - UFAL, Instituto de Química e Biotecnologia, 57072-970, Maceió, AL, Brazil

Received: December 12, 2016; Revised: December 09, 2017; Accepted: December 11, 2017

The conditions of chemical synthesis can be crucial for polymerization of styrene in such a way that it can be produced latex beads at nanometric range ($\phi < 400\text{nm}$). In this work, it will be analyzed how the absence of N₂ and surfactant will result in colloidal particles with high affinity to agglomerate forming two kinds of nanostructured assemblies: colloidal crystals and nanowires. Four syntheses were realized and four parameters were changed: temperature, impeller speed, and initiator and styrene concentrations. The dispersion was filtered and coated on glass slides by evaporation induced self-assembly (EISA) process. Morphology and topography were observed at Scanning Electron Microscopy (SEM) and Atomic Force Microscope (AFM) respectively. They show how the synthesis conditions play a vital role on the formation of self assembly nanostructures that can be applied as templates for sensors and biomaterials devices.

Keywords: *polymerization, nanowires, colloidal particles, surface characterization.*

1. Introduction

Nanoscience has opened new routes for nanoparticle synthesis that became possible the preparation of different metallic and nonmetallic materials. These new materials are essentially constituted by colloidal particles with modifications in their surface. Such particles can be functionalized with functional groups such as carboxylates, ammonia or oligo ethylene glycol¹. Nanoparticles suffer induced changes in their surfaces generating different morphologies and topographies from self-assembly monolayers (SAM) to bulk materials.

Two morphologies have been particularly reported in the literature: nanowires and monodisperse spheres. Nanowire has different technological applications ranging from microelectronics to biomaterials²⁻⁸. However, self assembly of nanowires involves more far-reaching interactions than those observed in spherical particles. In general, it is observed the need to charge electrically or magnetically the surface of nanowire in such a way that there will be the alignment of this structure when subjected to the application of an electromagnetic field. The behavior of self assembly quantum wires can be very difficult to describe. The reason is that several effects are involved in their formation and arrangement. Therefore, quantum size effects, high surface area and low influence of gravity must not be ignored.

Vapor-liquid-solid process is one of the most common methods for nanowire synthesis⁹. Such method has been used for the growth of silicon nanowires wherein the presence of nano droplets of Fe-Si in a silicon vapor saturated environment leads to nanowire growth. This structure shows a vertical growth orientation perpendicular to the plane [111] of silicon crystal lattice. The orientation of the nanowires will depend on two different factors: nano drop size and energetic interactions of the surface. Polymers can also be generated in the form of nanowires by electrospinning. The technique is based on the application of an electric field in a polymer solution inside a metallic capillary^{10,11}. This process allows obtaining polymeric wires in monolayers or multilayers with different compositions and thicknesses. Carbon nanowires morphology has been originally described in nanoscience since the original work of Iijima that obtained carbon nanotubes from graphite sheets¹²⁻¹⁴. Several other processes have been reported in the literature to produce carbon nanotubes such as high electrical energy application and chemical vapor deposition (CVD)^{15,16}. Carbon nanotubes have electrical and mechanical properties that differ from those found in graphite such as electrical conductivity, thermal and mechanical resistance.

Silica and latex have been widely reported in the literature as templates for porous materials. Synthesis of spherical particles with well defined size has also been the object of research, due to its application in the field of

*e-mail: djalmeno@gmail.com

photonic crystals, sensors and solar cells¹⁷⁻²⁰. Beads can be synthesized in different sizes at nanometric scale and support high temperature and pressure conditions making them ideal for preparation of semiconductor materials. Silica beads were originally obtained by Stöber method based on the hydrolysis and condensation of the tetraethylorthosilicate in the presence of ethanol and ammonia²¹. This synthesis route occurs via LaMer method in which nucleation happens rapidly in a single mode^{22,23}. These nuclei induce the aggregation of smaller particles that retain the spherical shape. Silica spheres are extensively applied in the chemical template of functional devices involving tri-dimensional photonic crystals²⁴⁻²⁶, solar cells²⁷ and sensors^{28,29}.

Spherical polymeric particles have been applied in nanotechnology because of their easy preparation and formation of self-structured arrangements with good definition at micrometric scale. There are reports in the literature of the use of polymer particles for the manufacture of photonic crystals³⁰, drug delivery systems³¹ and solar cells³² based on their ability to form self structured arrangements in the size scale required for that application. Polystyrene has been one of the most widely used polymers in the preparation of these nanomaterials since the original work of Holland et al.^{33,34}. In these reports, it has been defined the first route to prepare porous oxides of Si, Ti, Zr, Al, W, Fe, Sb, and a mixture of Zr/Y in a single step reaction with polystyrene beads. Conventional self assembly techniques such as centrifugation, sedimentation and EISA have been used to analyze how latex beads can form templates. This technique has been successfully applied for porous silica and synthesis conditions (temperature, concentration of the reactants and impeller rotation) have been directly related to the morphology and topography after analysis by MEV characterization techniques³⁵.

In this work, it is discussed the formation of spherical latex particles in aqueous medium without the presence of surfactant and oxygen inside a cylindrical vessel. Four syntheses were performed and four parameters were varied: temperature, rotation and concentration of the reactants (monomer and initiator). Self-assembly was performed by EISA technique and particles morphology was determined by SEM. It is observed that there is a strong tendency of agglomeration of these particles particularly when coated on metallic substrates. The same technique was used in glass substrates and it was observed by AFM technique the formation of aligned wires in a preferential orientation due to the action of capillary forces. Self-assembly of latex beads in nanowires is associated to the action of capillary forces defining a crystallographic orientation. Other trend is that the charge surface induces coalescence process forming a continuous and well defined cylindrical configuration present at latex beads prepared in this work. Therefore, these results show that latex beads can be synthesized without N₂ gas and they can be coated on substrate resulting in nanowires which

can be applied as templates for manufacture of photonic crystals and biosensors.

2. Method and Procedure

2.1 Synthesis of latex beads

Synthesis of polystyrene beads was carried out according to the procedures described by Holland et al.³⁴. However, some modifications have been made regarding the geometry of the vessel and the conditions of the synthesis. Figure 1A shows the container used in the synthesis of latex beads. This is a low-cost commercial glass jar and a polyacetate cover with three inputs for thermometer, condenser and liquid inlet or outlet from the vessel. There is also one central input for the agitator rod and two lateral valves for gas inlet or outlet. This flask was placed on a magnetic stirrer and heater (GEHAKA, Model AA-2050) and mechanically fixed by the stem of the digital mechanical stirrer (GEHAKA, Model AM-20).

The reagents used for the synthesis of the latex beads were only styrene monomer and potassium persulfate from Sigma Aldrich. Each synthesis was performed with variations in four parameters: temperature, impeller speed and concentration of the initiator or monomer as shown in Table 1. Four syntheses were carried out and labeled with Roman numeral. Temperature of dispersion was varied in the range from 60 to 90 °C and it is directly related to polymerization rate of styrene monomer. Only two values have been used to change the rotation impeller of the dispersion. They are 300

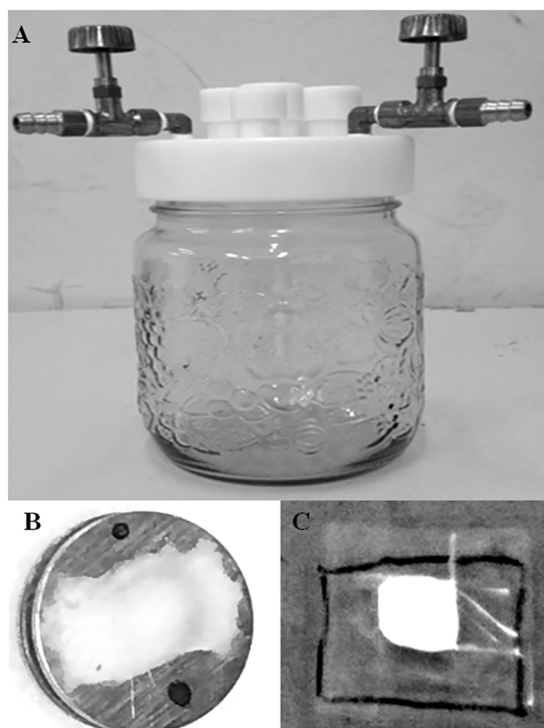


Figure 1. Synthesis of latex beads: (A) - cylindric flask; (B) - film coated at metallic substrate; (C) - film coated at glass substrate.

Table 1. Parameters for synthesis of latex beads.

SYNTHESIS	TEMPERATURE(°C)	ROTATION(RPM)	INICIATOR CONCENTRATION(g/L)	STYRENE VOLUME (mL)	YIELD (%)
I	85	600	0.9653	75	12
II	80	600	0.9634	75	97
III	68	300	0.3329	50	16
IV	70	300	1.6019	100	62

and 600 RPM in order to see how the increase of impeller speed can modify the synthesis yield. The synthesis yield was calculated considering the density of styrene as 0.9016 g/mL³⁶. It has been determined after the dry of a fixed volume of dispersion and weighing the mass of latex beads labeled as *m*. It has been considered the expected mass of latex beads to be obtained in total volume of dispersion labeled as *M_T*. The ratio *m* by *M_T* corresponds to synthesis yield. Other parameters are responsible for the formation of latex beads as initiator concentration that induces the polymerization process and styrene volume that must be adjusted to increase latex beads concentration in the dispersion. Synthesis I had the lower yield while synthesis II had the higher yield. The yield range was from 10 to 90% showing that it is possible to adjust it only by the control of temperature and initiator concentration. Synthesis was initiated by introducing 900 mL of Mili-Q water into the vessel. Temperature of the dispersion was fixed through a thermocouple interconnected to the digital heater. Once the desired temperature was reached, styrene was added with water in constant agitation. Synthesis was performed without the injection of N₂, although the vessel remained isolated from the environment by the polyacetate cover. It was observed that the dispersion assumed a white coloration which is characteristic of the dispersion of light by the colloidal particles and indicated the formation of a polymeric chain. Potassium persulfate solution was slowly introduced for 1 hour whose concentration was specific to each synthesis. The end of the synthesis occurred after four hours from the beginning. The dispersion was allowed to stand and cooled to room temperature for 24 hours. After this period, the dispersion was filtered on standard filter paper to prevent the formation of agglomerates and stored in the refrigerator.

2.2. Films generation

Some drops of the dispersion at Petri plate were dried at room environment and a white powder was formed. This material was characterized by Thermogravimetric Analysis (TGA) and Differential Thermogravimetric Analysis (dTGA). The equipment was from Shimadzu, model TGA-51H (MACRO TG). Similar procedure was performed in order to determine the yield of the polymerization calculating the ratio of mass for the powder compared to the original mass of styrene.

Latex beads were characterized by MEV through the formation of films by EISA process. The dispersion was diluted in water at a concentration of 10% V/V₀. Two types of films were produced according to the type of substrate (metal or glass). The first type of substrate was metallic corresponding to the sample holder of the scanning electron microscope. Some drops of the dispersion was spread on the metallic substrate and dried at room environment. The films have been labeled as SHI, SHIII and SHIV. Figure 1B shows the appearance of the film at metallic substrate. It is dense, opaque and mechanically unstable. The second substrate is an optical microscope blade. This second substrate was coated with durex to define a central area of approximately 1cm². It is thus ensured that the evaporation of the dispersion would occur in a predetermined area without draining at the borders. A few drops of the dispersion were added with a plastic pipette; the liquid was spread and allowed to dry during 30 minutes. This procedure was performed on a heating plate with two pairs of Petri dishes. One of the plate contained water and thermocouple serving as reference for heater temperature. Other pair of Petri dish was used as a vessel for the generation of films by EISA process. There was evaporation of the solvent at 50° C and formation of a clear film after 30 minutes. The appearance of the films coated on glass substrate is shown at Figure 1C. They are also dense, opaque and mechanically unstable. It was observed for some films the appearance of colored reflections of red or green tones according to the incidence of light. The films have been labeled as GSI, GSII GSIII and GSIV.

2.3. Surface Characterization

Scanning electron micrographs were obtained with a Shimadzu VEGA3 chamber type LM with a conventional tungsten heated cathode intended for high vacuum operations with secondary electron detectors (SE) and backscattered electron detectors (BSE) apparatus, after gold metallization (Quorum Technologies LTD, Ashford, model Q15OR). The sample was broken into a piece of area smaller than 50mm² which was subsequently taken to gold evaporator. The deposition of gold lasted for approximately 10 min and a homogeneous conductive layer was formed. The film was taken to a vacuum chamber and subjected to electron beam scanning to characterize its surface in terms of morphology and topography surface. Only films from synthesis II have

been characterized by AFM before SEM measurement. AFM measurements have been realized at the bare substrate and at latex bead film. AFM equipment was from Shimadzu, Model SPM-9700. After AFM measurement, latex beads film has been analyzed by SEM in order to assure that same topography profile was obtained in different surface characterization techniques.

3.Result and Discussion

Figure 2 shows thermal behavior of latex beads obtained by TGA technique. It can be seen that latex beads have only one region of mass loss from 200°C to 500°C. This loss is associated to thermal decomposition of polystyrene by combustion generating water and CO₂. Mass loss is around 93.53% after 500°C and there is no change for higher temperatures. DrTGA shows that mass loss rate becomes significant at 340°C reaching the maximum at 425°C. These temperatures are far away from those used to form the film by EISA technique. Therefore, it will be expected that film topography will not be changed directly by temperature.

Figure 3 shows how the coating of latex beads can be very different depending on the conditions of deposition. It can be seen that it is possible to obtain a dense film if deposition happens without any restriction of the spreading of latex beads (Figure 3A). It is not expected dense film for metallic substrate. The formation of dense films can be associated to high surface potential over latex beads synthesized at more high temperature and impeller speed. These factors can avoid the formation of polymeric chain necessary to grow latex beads. The initiator concentration tends to increase in polymeric particles and small particles are generated along the dispersion. These particles have a strong surface potential and it is expected that coalescence processes are more effective to form dense films. It can be seen that the behavior is completely different if there is restriction during EISA process (Figure 3B). There is the formation of nanowires not well defined but showing that they are separated forming a cylindrical topography along the

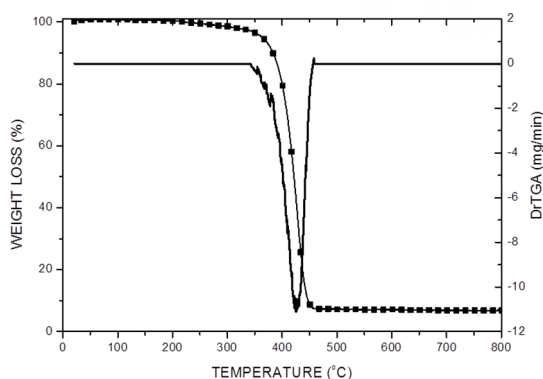


Figure 2. Thermogravimetric analysis TGA and drTGA for latex beads.

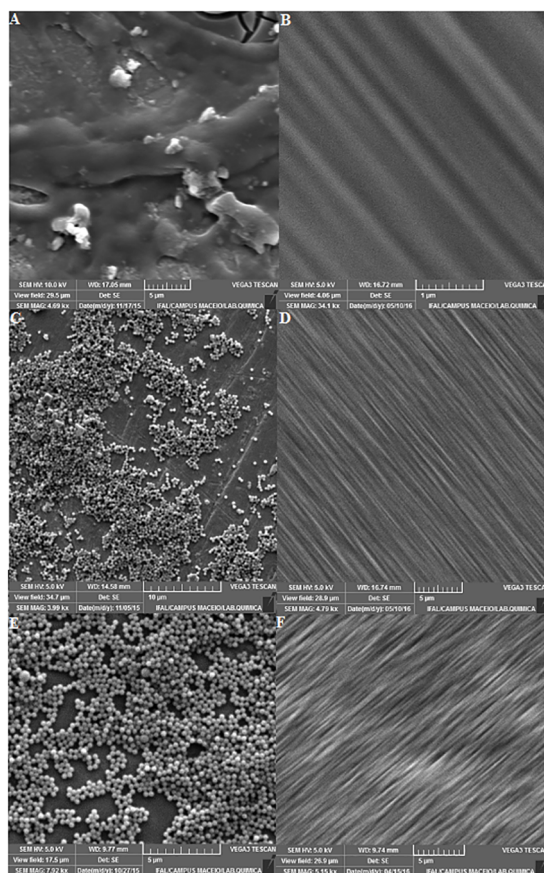


Figure 3. SEM microphotographies of latex beads films: (A) - SHI; (B) - GSI; (C) - SHIII; (D) - GSIII; (E) - SHIV; (F) - GSIV.

substrate. It can be seen at Figure 3C that isolated particles can be spread on the substrate and it can be inferred that their diameter is close to 400 nm. In this case, the formation of nanowire is not complete and it can be observed at Figure 3D little needles along the substrate. This film corresponds to Synthesis III whose yield was low (~16%). The increase of synthesis yield did not change the particle morphology as it can be seen at Figure 3E. The same nanowire topography is observed when the particles were coated by EISA process at glass substrate (Figure 3F). These results show that these particles tend to aggregate covering the substrate forming a typical cylindrical architecture whose definition will depend essentially on their mutual interaction. The main objective to obtain latex beads films on different substrates is that the behavior is completely different from that usually expected for commercial latex beads. It can be seen that latex beads tend to form isolated centers over metallic substrate but there is a clear tendency to form clusters. The metallic substrate should present a more effective spreading of latex beads along the surface because contact angle is smaller than glass substrate. Latex beads should be distinguished in glass substrate but the deposition conditions are different in two features: restricted area for latex beads spreading and

temperature control. It can be seen that latex beads has a preferential alignment due to action of capillary forces but there is also a strong electrostatic interaction among the particles. This leads to coalescence processes and the final result is the generation of nanowires.

The highest yield happens for Synthesis II (~97%) and films morphology determined by SEM characterization is shown at Figure 4. It is observed that the film covers completely the substrate and some regions shows some stripes which resemble wires with a preferential alignment (Figure 4A). There are also cracks due to low adherence of latex beads along the substrate. Figure 4B shows that nanowires extend over a large area (0.25mm²) forming well defined crystallographic domains over the substrate. Nanowires have preferential alignment as it can be seen at Figure 4C due to action of capillary forces. There is some discordance along the surface but it has not been observed for this film any change in the preferential direction of nanowires growth. This result shows that nanowires not only grow horizontally along the substrate but also their alignment is homogeneous over whole surface. Figure 4D shows how the films morphology is well defined. Nanowires have a typical cylindrical morphology with diameter estimated at 400 nm and with pore spacing close to 100 nm.

AFM characterization of latex beads film is shown at Figure 5. It can be seen that bare substrate does not show any regular surface pattern (Figure 5A) and it can be considered a flat surface with small variation below 100nm. There are some isolated cracks along the surface but the surface is plane with some little grains whose size can be considered lower than 30 nm for area scan of 4.0 μm² displayed at Figure 5B. Surface topography for latex beads film is

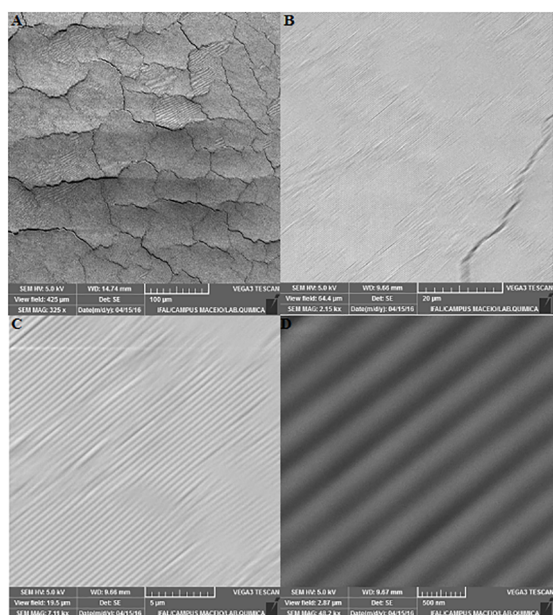


Figure 4. SEM microphotographies of latex beads film GSII at different magnifications: (A) - 325x; (B) - 2150x; (C) - 7110x; (D) - 48200x.

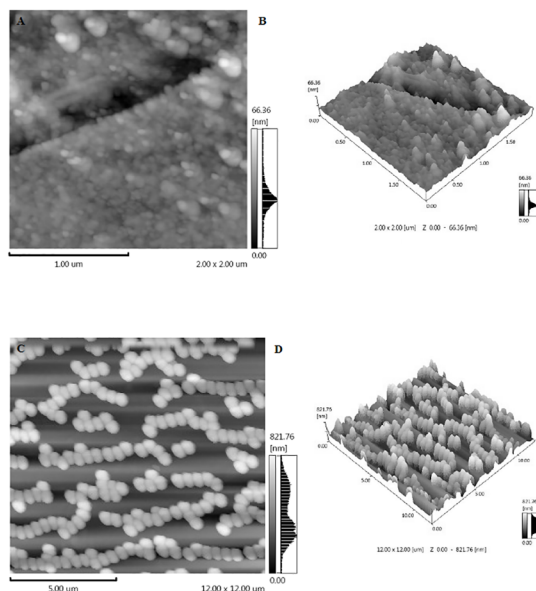


Figure 5. AFM characterization of latex beads films: (A) - bare substrate (surface profile); (B) - bare substrate (3-dimension profile); (C) - GSII (surface profile); (D) - GSII (3-dimension profile)

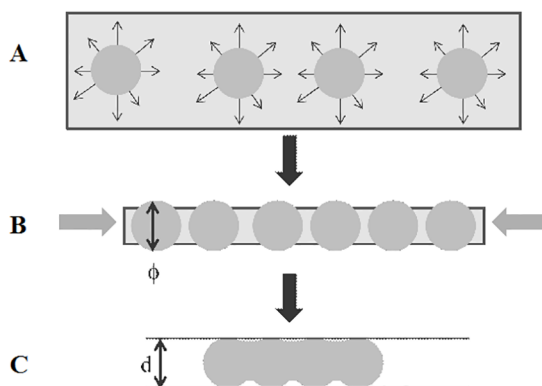


Figure 6. Scheme for the formation of nanowires of latex films by EISA process: (A) - intermolecular forces in the dispersion; (B) - action of capillary force during EISA process; (C) - consolidation of nanowires by coalescence process. ϕ = particle diameter; d = nanowires diameter.

shown at Figure 5C where it can be seen a regular pattern of fringes along whole substrate. There is agglomeration of particles between the fringes and the spherical shape is lost. However, it can be seen that these particles tend to follow the same alignment of the fringes forming ribbons above the film surface. Figure 5D shows 3-dimension profile of latex bead film for 12μmx12μm area. It can be seen that fringes have size around 400nm very close to latex beads diameter.

The experimental results show that there is the polymerization of styrene due to presence of initiator. Beads are produced as it can be seen at Figures 3C and 3E, however they have a strong tendency to combine associated to their surface charge. Table I shows that this trend happens during the synthesis. Synthesis I and II has similar conditions and a decrease of 5 °C at temperature result in a strong increase of

synthesis yield (~97%). Similar behavior can be observed for synthesis III and IV, however mass of reagents is responsible for the increase of yield from 16% to 62%. Barros et al.³⁵ report for latex beads synthesized at spherical flask that rotation can induce two kinds of latex beads with different sizes and how this morphology can change the topography of macroporous silica. It is expected for this new synthesis route that small variation of synthesis parameters can result in fast polymerization of styrene due to absence of N₂ gas and surfactant in the dispersion during the synthesis. Anionic and cationic surfactants are directly responsible for the stability and growth of latex beads. Gu et al. reported that micron-size polymeric particles can be obtained by the control of aggregation and dispersion stability of polymeric particles by addition of cationic (CTAB - cetyltrimethylammonium bromide) and anionic (SDS - sodium dodecyl sulfate)^{37,38} surfactants. This is a single stage polymerization technique at which the negative charge of the potassium persulfate initiator is neutralized by cationic surfactant stopping the aggregation process. After reaching a certain size value, anionic surfactant is added in such a way that microsized particle can be achieved. N₂ gas is commonly used to remove oxygen of water in such way that there is not an increase of negative charge over the polymeric particle which could lead to aggregation process during the synthesis and consequently non-homogenous particle size distribution will result after the end of polymerization process. The main effect of the absence of N₂ and surfactant during synthesis process consists on the increase of latex beads surface charge. This trend leads to particle coalescence which can be preferentially directed during EISA process. It can be seen that two factors act during film generation: capillary force and electrostatic interaction. Thus nanowires arrangement happens specifically for latex beads generated without surfactant and N₂. The main effect of the absence of N₂ and surfactant during synthesis process consists on the increase of latex beads surface charge. This trend leads to particle coalescence which can be preferentially directed during EISA process. It can be seen that two factors act during film generation: capillary force and electrostatic interaction. Thus nanowires arrangement happens specifically for latex beads generated without surfactant and N₂.

Figure 6 shows how the formation of nanowires happens during EISA process. It can be seen that the particles are stable at dispersion and they do not join because there are repulsive surface electrostatic interactions acting among them (Figure 6A). This repulsive interaction is associated to SO⁴⁻ anions from the initiator present at polystyrene surface. The solvent evaporation during EISA process induces to the approximation of latex beads by the action of capillary forces (Figure 6B). This process is more intense when solvent thickness is the same order of particle diameter (ϕ) and spheres concentration is appropriate to cover completely the substrate. At the end, drop coalescence process happens and spherical surface is lost (Figure 6C) generating cylindrical nanowires with

diameter d defined by the original latex beads synthesized in this new chemical route. This new approach can be extended to control the size of latex beads and consequently the diameter of nanowires. It can be obtained small particles by remotion of aliquots during synthesis and subsequent elimination of styrene excess at 70°C by evaporation at open air. This procedure could result in nanometric nanowires for nanofilters or catalyzers. Other procedure consists on the synthesis with original polymeric particles. They will attach oligomers generated during polymerization reaction and will grow into micrometric scale. This procedure is under way in order to create huge hollow oxide microtubes to be applied in solar cells and chemical sensors.

4. Conclusion

The experimental results of this work show that it is possible to produce latex beads at cylindrical flask with a low cost infrastructure and without N₂ gas. Particles size is close to 400nm for all syntheses, but their polymerization process depends mainly on temperature and reagent concentrations. Latex beads have also strong tendency to agglomerate generating dense films or nanowires depending on their concentration along the substrate. These nanowires are formed by the action of capillary forces acting horizontally in a restrict area along the substrate. It is obtained a cylindrical topography whose size scale is determined by the original latex beads synthesized in this work. The experimental results also show that is possible to obtain a cylindrical topography for latex beads independent of the synthesis conditions. However, there is a strong tendency to particles aggregation associated intrinsically to their surface potential. Dense films can be easily formed especially at metallic substrate where the spreading of latex beads is more effective. The main contribution of this work is to show that EISA process can be applied to formation of self assembly films with two forces acting directly for the formation of cylindrical nanowires. Firstly, capillary forces align horizontally latex beads and simultaneously electrostatic interaction leads to coalescence process. This will be possible solely because solvent evaporation rate happens in a controlled way and there is restriction for the spreading of latex beads. It is possible that this new approach can be used at different substrates and at a wide range of size scale for latex beads. This new self-assembly for latex beads can be very interesting for generation of oxides tubes to be applied at bi-dimensional photonic crystals, chemical sensor and biomaterials.

5. Acknowledgements

D. A. Barros Filho acknowledges the financial support of Conselho Nacional de Desenvolvimento Científico e Tecnológico - CNPq - Brasil (Process Number: 487978/2013-7/CNPq).

6. References

1. Wuelfing WP, Gross SM, Miles DT, Murray RW. Nanometer Gold Clusters Protected by Surface-Bound Monolayers of Thiolated Poly(ethylene glycol) Polymer Electrolyte. *Journal of the American Chemical Society*. 1998;120(48):12696-12697. DOI: 10.1021/ja983183m
2. Du J, Li X, Li K, Gu X, Qi W, Zhang K. High hydrophilic Si-doped TiO₂ nanowires by chemical vapor deposition. *Journal of Alloys and Compounds*. 2016;687:893-897. DOI: 10.1016/j.jallcom.2016.06.182
3. Feng Q, Liu J, Yang Y, Pan D, Xing Y, Shi X, et al. Catalytic growth and characterization of single crystalline Zn doped p-type β -Ga₂O₃ nanowires. *Journal of Alloys and Compounds*. 2016;687:964-968. DOI: 10.1016/j.jallcom.2016.06.274
4. Hui N, Sun X, Song Z, Niu S, Luo X. Gold nanoparticles and polyethylene glycols functionalized conducting polyaniline nanowires for ultrasensitive and low fouling immunosensing of alpha-fetoprotein. *Biosensors and Bioelectronics*. 2016;86:143-149. DOI: 10.1016/j.bios.2016.06.028
5. Hou NY, Zhu J, Zhang H, Perinpanayagam H. Epoxy resin-based ultrafine dry powder coatings for implants. *Journal of Applied Polymer Science*. 2016;133(37):43960. DOI: 10.1002/app.43960
6. Jayaramudu T, Raghavendra GM, Varaprasad K, Reddy GVS, Reddy AB, Sudhakar K, et al. Preparation and characterization of poly(ethylene glycol) stabilized nano silver particles by a mechanochemical assisted ball mill process. *Journal of Applied Polymer Science*. 2015;133(7):43027. DOI: 10.1002/app.43027
7. Lizundia E, Ruiz-Rubio L, Vilas JL, León LM. Poly(l-lactide)/zno nanocomposites as efficient UV-shielding coatings for packaging applications. *Journal of Applied Polymer Science*. 2015;133(2):42426. DOI: 10.1002/app.42426
8. Rezaee A, Pourtagi G, Hossini H, Loloi M. Microbial cellulose as a support for photo-catalytic oxidation of toluene using TiO₂ nanoparticles. *Journal of Applied Polymer Science*. 2016;133(8):43051. DOI: 10.1002/app.43051
9. Morales AM, Lieber CM. A Laser Ablation Method for the Synthesis of Crystalline Semiconductor Nanowires. *Science*. 1998;279(5348):208-211. DOI: 10.1126/science.279.5348.208
10. Jalili R, Morshed M, Ravandi SAH. Fundamental parameters affecting electrospinning of PAN nanofibers as uniaxially aligned fibers. *Journal of Applied Polymer Science*. 2006;101(6):4350-4357. DOI: 10.1002/app.24290
11. Li D, Wang Y, Xia Y. Electrospinning Nanofibers as Uniaxially Aligned Arrays and Layer-by-Layer Stacked Films. *Advanced Materials*. 2004;16(4):361-366. DOI: 10.1002/adma.200306226
12. Iijima S. Helical microtubules of graphitic carbon. *Nature*. 1991;354(6348):56-58. DOI: 10.1038/354056a0
13. Iijima S. Growth of carbon nanotubes. *Materials Science and Engineering: B*. 1993;19(1-2):172-180. DOI: 10.1016/0921-5107(93)90184-O
14. Iijima S, Ichihashi T. Single-shell carbon nanotubes of 1-nm diameter. *Nature*. 1993;363(6430):603-605. DOI: 10.1038/363603a0
15. Little RB. Mechanistic Aspects of Carbon Nanotube Nucleation and Growth. *Journal of Cluster Science*. 2003;14(2):135-185. DOI: 10.1023/A:1024841621054
16. Rao CNR, Govindaraj A. Carbon nanotubes from organometallic precursors. *Accounts of Chemical Research*. 2002;35(12):998-1007. DOI: 10.1021/ar0101584
17. Kurdyukov DA, Eurov DA, Stovpiaga EY, Yakovlev SA, Kirilenko DA, Golubev VG. Photonic crystals and glasses from monodisperse spherical mesoporous silica particles filled with nickel. *Physics of the Solid State*. 2014;56(5):1033-1038. DOI: 10.1134/S1063783414050138
18. Trofimova EY, Kurdyukov DA, Yakovlev SA, Kirilenko DA, Kukushkina YA, Nashchekin AV, et al. Monodisperse spherical mesoporous silica particles: Fast synthesis procedure and fabrication of photonic-crystal films. *Nanotechnology*. 2013;24(15):155601. DOI: 10.1088/0957-4484/24/15/155601
19. Hashimoto M, Inoue H, Hyodo T, Shimizu Y, Egashira M. Preparation and Gas Sensor Application of Ceramic Particles with Submicron-Size Spherical Macropores. *Sensor Letters*. 2008;6(6):887-890. DOI: 10.1166/sl.2008.524
20. Grandidier J, Callahan DM, Munday JN, Atwater HA. Light Absorption Enhancement in Thin-Film Solar Cells Using Whispering Gallery Modes in Dielectric Nanospheres. *Advanced Materials*. 2011;23(10):1272-1276. DOI: 10.1002/adma.201004393
21. Stöber W, Fink A, Bohn E. Controlled growth of monodisperse silica spheres in the micron size range. *Journal of Colloid and Interface Science*. 1968;26(1):62-9. DOI: 10.1016/0021-9797(68)90272-5
22. LaMer VK, Dinegar RH. Theory, Production and Mechanism of Formation of Monodispersed Hydrosols. *Journal of the American Chemical Society*. 1950;72(11):4847-4854. DOI: 10.1021/ja01167a001
23. Matijevic E. Preparation and properties of uniform size colloids. *Chemistry of Materials*. 1993;5(4):412-426. DOI: 10.1021/cm00028a004
24. Huang WH, Shieh JM, Pan FM, Shen CH, Lien YC, Tsai MA, et al. UV-Visible Light-Trapping Structure of Loosely Packed Submicrometer Silica Sphere for Amorphous Silicon Solar Cells. *IEEE Electron Device Letters*. 2012;33(7):1036-1038. DOI: 10.1109/LED.2012.2196974.
25. Chaouachi A, Radhouane C, M'Nif A, Hamzaoui AH. Optical simulation of colloidal photonic crystals with controllable size spheres of silica. *European Physical Journal Applied Physics*. 2014;67(3):30501. DOI: 10.1051/epjap/2014140079
26. Deng TS, Zhang JY, Zhu KT, Zhang QF, Wu JL. Temperature-modified photonic bandgap in colloidal photonic crystals fabricated by vinyl functionalized silica spheres. *Materials Chemistry and Physics*. 2011;129(1-2):540-546. DOI: 10.1016/j.matchemphys.2011.04.064
27. Jiang Q, Gao J, Tao H, Fang G, Wei H, Yi L. Enhanced performance of dye-sensitized solar cells using silica/gold core-shell spheres modified photoanodes. *Materials Letters*. 2014;134:16-19. DOI: 10.1016/j.matlet.2014.07.007

28. Haro-González P, Martínez Maestro L, Trevisani M, Polizzi S, Jaque D, García Sole J, et al. Evaluation of rare earth doped silica sub-micrometric spheres as optically controlled temperature sensors. *Journal of Applied Physics*. 2012;112(5):054702. DOI: 10.1063/1.4751349
29. Li X, He G, Han Y, Xue Q, Wu X, Yang S. Magnetic titania-silica composite-Polypyrrole core-shell spheres and their high sensitivity toward hydrogen peroxide as electro-chemical sensor. *Journal of Colloid and Interface Science*. 2012;387(1):39-46. DOI: 10.1016/j.jcis.2012.07.071
30. Ding C, Hu JC, Yuan W, Du DZ, Yang Y, Chen G, et al. Facile fabrication of centimeter-scale stripes with inverse-opal photonic crystals structure and analysis of formation mechanism. *RSC Advances*. 2016;6(60):54976-54983. DOI: 10.1039/C6RA07314J
31. Liu L, Liu M, Dong Y, Zhou W, Zhang L, Su Y, et al. Preparation, heat-enabled shape variation, and cargo manipulation of polymer-based micromotors. *Journal of Materials Science*. 2016;51(3):1496-1503. DOI: 10.1007/s10853-015-9470-6
32. Yang SC, Yang DJ, Kim J, Hong JM, Kim HG, Kim ID, et al. Hollow TiO₂ Hemispheres Obtained by Colloidal Templating for Application in Dye-Sensitized Solar Cells. *Advanced Materials*. 2008;20(5):1059-1064. DOI: 10.1002/adma.200701808
33. Holland BT, Blanford CF, Stein A. Synthesis of Macroporous Minerals with Highly Ordered Three-Dimensional Arrays of Spheroidal Voids. *Science*. 1998;281(5376):538-540. DOI: 10.1126/science.281.5376.538
34. Holland BT, Blanford CF, Do T, Stein A. Synthesis of Highly Ordered, Three-Dimensional, Macroporous Structures of Amorphous or Crystalline Inorganic Oxides, Phosphates, and Hybrid Composites. *Chemistry of Materials*. 1999;11(3):795-805. DOI: 10.1021/cm980666g
35. Barros Filho DA, Hisano C, Bertholdo R, Schiavetto MG, Santilli C, Ribeiro SJL, et al. Effects of self-assembly process of latex spheres on the final topology of microporous silica. *Journal of Colloid and Interface Science*. 2005;291(2):448-464. DOI: 10.1016/j.jcis.2005.05.016
36. Haynes WM, ed. *CRC Handbook of Chemistry and Physics*. 94th ed. Boca Raton: CRC Press; 2013.
37. Gu S, Mogi T, Konno M. Preparation of Monodisperse, Micron-Sized Polystyrene Particles with Single-Stage Polymerization in Aqueous Media. *Journal of Colloid and Interface Science*. 1998;207(1):113-118. DOI: 10.1006/jcis.1998.5768
38. Gu S, Mogi T, Konno M. Single stage polymerization technique for producing monodisperse micron-size polymer particles. *Colloids and Surfaces A: Physicochemical and Engineering Aspects*. 1999;153(1-3):209-213. DOI: 10.1016/S0927-7757(98)00444-0